

Vibrational properties versus on- and off-axis behavior of the $F_A(\text{Li}^+)$ center in alkali halides

M. Leblans, W. Joosen,* and D. Schoemaker

Physics Department, University of Antwerp (U.I.A.), Universiteitsplein 1, B-2610 Wilrijk (Antwerp), Belgium

(Received 22 May 1990)

The polarized resonant Raman spectra of the $F_A(\text{Li}^+)$ center in several alkali halides are interpreted by means of a behavior-type analysis. This yields the defect symmetry and the representation of the observed vibrational modes. It is found that in a given host lattice the on- or off-center behavior of the isolated Li^+ center is systematically preserved on perturbing it with a nearest-neighbor F center. The Raman spectra of the off-axis $F_A(\text{Li}^+)$ centers exhibit both the Li^+ vibrations perpendicular and parallel to the defect axis. For the on-axis centers, only the latter is observed. The occurrence of high-frequency Li^+ modes for both on- and off-axis centers is related to a displacement of the Li^+ equilibrium position parallel to the defect axis and, due to the small impurity size, away from the adjacent F center. The occurrence of high-frequency Li^+ modes is attributed to ionic relaxation of the impurity and/or its nearest neighbors. This is in agreement with the theoretically calculated *high-frequency* Li^+ modes for the off-center Li^+ impurity in KCl and with the observation of *low-frequency* localized modes for the isolated Li^+ impurity with on-center behavior. The frequencies of the lowest vibrational levels in the off-axis system $\text{RbCl}:F_A(\text{Li}^+)$ are very close to those of the harmonic approximation. This is in contrast to the strongly anharmonic Li^+ potential, which was established for the isolated on-center Li^+ in KBr.

I. INTRODUCTION

It has been shown for KCl that the off-center behavior of the isolated Li^+ impurity remains, when it is perturbed by a nearest-neighbor (NN) F center, resulting in the formation of an $F_A(\text{Li}^+)$ center.¹⁻³ A correlation was suggested between the off-center and tunneling behavior of an F_A center, on the one hand, and its being type II, on the other hand.^{4,5} $F_A(\text{II})$ -type centers are distinguished from $F_A(\text{I})$ -type centers by a larger Stokes shift of the emission band and by their temperature-independent efficient optical reorientation.^{5,6} Most of the experimental techniques can only probe the off-center position of impurity ions, when they are mobile between the equivalent off-center potential minima. For this reason, no paraelectric cooling was observed for the nonreorienting isolated Li^+ impurity in RbCl at low temperatures.⁷ By means of the temperature dependence of dielectric measurements, Thörmer and Lüty demonstrated that the isolated Li^+ impurity in RbCl freezes in already below 42 K.⁴ The transition from $F_A(\text{II})$ - to $F_A(\text{I})$ -type center for $\text{RbCl}:F_A(\text{Li}^+)$ was related to the freezing of the Li^+ ion in one of the off-center positions with decreasing temperature.⁵ These suggestions are based on the assumption that the on- or off-center behavior of an isolated impurity is preserved for the F_A center, which is, at present, only explicitly verified for $F_A(\text{Li}^+)$ in KCl and KBr.^{1-3,8} Considering the extreme sensitivity of the Li^+ potential to the lattice parameter^{9,10} and to additional perturbations in its environment,⁸ straightforward comparison of the Li^+ and the $F_A(\text{Li}^+)$ centers is not *a priori*

evident.

The isolated off-center Li^+ in KCl possesses an infrared- and Raman-active mode at 43 cm^{-1} with an anomalous isotope shift.^{11,12} Both from a theoretical study¹³ and from the analysis of the polarized Raman spectra¹⁴ it was demonstrated that the Li^+ ion barely participates in this mode, in contrast to its initial interpretation.¹¹ High-frequency Li^+ vibrations were calculated for $\text{KCl}:\text{Li}^+$ to be at 280 and 380 cm^{-1} . Whereas such vibrations have never been observed for the isolated impurity center, the Raman spectra of $F_A(\text{Li}^+)$ exhibit high-frequency Li^+ modes.^{1,3,8,12} The 266 - and 216-cm^{-1} modes in $\text{KCl}:F_A(\text{Li}^+)$ are attributed to a Li^+ motion parallel and perpendicular to the defect axis, respectively, both within the C_{1h} mirror plane of the off-axis model.³ For $\text{KBr}:F_A(\text{Li}^+)$, in which the Li^+ ion is positioned on axis, only a single high-frequency mode is observed, corresponding to a Li^+ vibration parallel to the F_A defect axis.⁸ In the infrared absorption spectrum of the on-center systems $\text{NaCl}:\text{Li}^+$ and $\text{KBr}:\text{Li}^+$, however, *low-frequency* Li^+ vibrations were observed at 43.7 and 16.3 cm^{-1} , respectively.¹¹ Furthermore, a low-frequency lattice mode, similar to the ones observed for the isolated Li^+ center in KCl and for $F_A(\text{Li}^+)$ in KCl and KBr,^{1,3,8,12} does not occur for the isolated Li^+ center in KBr.

This paper presents a systematic investigation of the $F_A(\text{Li}^+)$ center in several alkali halides by means of the polarized resonant Raman-scattering technique. After the experimental details (Sec. II), the polarized Raman spectra of $F_A(\text{Li}^+)$ in RbCl, NaCl, and KF are presented

in Sec. III. The interpretation of the measurements is based on a behavior-type (BT) analysis (Sec. IV), which yields, within clearly spelled-out limits, the defect symmetry and the representation of the observed vibrational modes.¹⁵⁻¹⁷ It was demonstrated in the investigation of the equilibrium orientation of molecular impurities that the method can be applied whether or not tunneling or classical reorientation occurs.^{18,19} The vibrational features of the $F_A(\text{Li}^+)$ center are summarized in Sec. V. The discussion is focused on the on- or off-axis behavior of $F_A(\text{Li}^+)$ and on the correlation between the equilibrium position of the Li^+ ion and the vibrational spectrum of the center. A comparison of the results of $F_A(\text{Li}^+)$ and those of the isolated Li^+ center is illuminating for the features of the localized Li^+ vibrations.

II. EXPERIMENTAL

The RbCl samples were supplied by ENEA (Centro Ricerche Energia Frascati). They were additively colored at 640 °C under 10 Torr potassium vapor. Potassium ions can be present in the crystals in a concentration comparable to Li^+ . For NaCl: Li^+ and KF: Li^+ x-ray irradiated crystals were used. 30-min x-ray irradiation was sufficient for NaCl, whereas for KF 3 h were needed to get high enough coloration. $F \rightarrow F_A$ conversion occurred near 250 K under F -light illumination. The crystals were pulled from melts containing 1 wt.% LiCl. The Li^+ isotope concentrations equal the natural abundance (93% $^7\text{Li}^+$). The Raman spectra of RbCl: $F_A(\text{Li}^+)$ were taken at temperatures ranging from 10 to 120 K, under excitation with the Kr^+ laser lines at 647.1, 676.4, and 752.5 nm. The absence of optical bleaching in the additively colored crystals permitted the use of laser output powers as high as 100 to 300 mW. For NaCl and KF the Raman spectra were recorded at 10 K under excitation with the Ar^+ laser lines in the range of 454.5 to 514.5 nm and with the 520.8- and 530.9-nm Kr^+ laser lines. The incident laser power varied between 20 and 50 mW. The resolution of the presented spectra is 2 cm^{-1} , unless otherwise indicated.

III. RAMAN SPECTRA OF $F_A(\text{Li}^+)$ IN RbCl, NaCl, AND KF

A. Intensity parameters and preferential orientation

The defect axis of $F_A(\text{II})$ -type centers, such as $F_A(\text{Li}^+)$ in RbCl and KF, exhibits fast reorientation upon optical excitation, even at low temperatures.^{5,6} Also for $F_A(\text{I})$ -type centers in x-ray irradiated samples reorientation at low temperatures has been observed.⁸ As a result, the centers are in general preferentially aligned during the Raman experiment. This means that the incident light acts as an *orientating operator*.¹⁵⁻¹⁷ The stationary distribution of the centers among their possible orientations depends crucially on the polarization and the wavelength of the incident light. For the scattering geometries used,

the orientating operator possesses a $D_4[100]$ symmetry group, if fast tunneling or hopping between the equivalent Li^+ potential minima is assumed in the case of an off-axis center.³

The BT analysis is based on the so-called intensity parameters (IP). The IP q , r , and s , which can be retrieved from the polarized Raman intensities $I_{\alpha,\beta}$, are²⁰

$$\begin{aligned} q_2 + s_{11} &= I_{yz,yz} + I_{y\bar{z},yz} , \\ r_1 + s_{12} &= I_{yz,yz} - I_{y\bar{z},yz} , \\ s_{21} &= I_{yz,x} , \end{aligned} \quad (1)$$

and

$$\begin{aligned} q_1 &= I_{x,x} , \\ s_{21} &= I_{x,y} . \end{aligned} \quad (2)$$

[cf. Figs. 2(a) and 2(b) in Ref. 3, respectively.] $I_{y\bar{z},yz}$, for example, denotes the scattered intensity polarized along the $[011]$ crystal direction, resulting from $[01\bar{1}]$ -polarized incident light. The distributions among the possible orientations of the centers, corresponding to (1) and (2), are different.³ A correct BT analysis, however, must be based on a set of IP, obtained from the same distribution of the centers. Set (1) will lead to more decisive conclusions than set (2), since more IP are retrieved from the polarized Raman data in this case. Since modes with nonzero s_i/q_i are observed, it is necessary to analyze the polarized Raman intensities by means of the extended tables of the BT method for resonant Raman scattering.^{20,21}

In the case of preferentially aligned centers, s_{11} , s_{12} , and s_{21} are in general not mutually equal. As a result, the IP q_2 and r_1 in Eqs. (1) cannot be obtained. This has important implications on the discriminative power of the BT analysis: e.g., in the case of an off-axis position of the Li^+ ion no distinction can be made between a Li^+ vibration parallel and perpendicular to the mirror plane of the C_{1h} symmetry. Preferential alignment of the $F_A(\text{Li}^+)$ centers may also result in preferential absorption of the scattered light: due to the optical anisotropy of the crystal, parallel and perpendicularly scattered light are differently absorbed. As a result, the *observed* polarization properties of the Raman spectra can differ from the actual ones. The effect is responsible for the discrepancies among the polarized Raman data of $F_A(\text{Li}^+)$ in KCl under F_{A1} excitation.³

In the case of an isotropic distribution of the centers, Eqs. (1) reduce to²¹

$$\begin{aligned} q &= I_{yz,yz} + I_{y\bar{z},yz} - I_{yz,x} , \\ r + s' &= I_{yz,yz} - I_{y\bar{z},yz} , \\ s &= I_{yz,x} ; \end{aligned} \quad (3)$$

since $q = q_i$, $r + s' = r_i + s_{i2}$, and $s = s_{i1} = s_{i3}$. This eliminates the technical difficulties in applying the BT analysis. Also, possible preferential absorption of the scattered light is avoided and it is not necessary to assume fast tunneling or hopping between the equivalent Li^+ potential minima in the case of an off-axis center, as was done for $F_A(\text{Li}^+)$ in KCl.³ The BT analysis of

$F_A(\text{Li}^+)$ in RbCl will therefore be based on the polarized Raman data under 676.4-nm excitation. At this wavelength the F_{A1} and F_{A2} transitions, which are mutually orthogonally polarized, absorb equally strongly, resulting in an equal distribution of the centers among their possible orientations. $F_A(\text{Li}^+)$ in NaCl has a random orientation under all excitations. Even at higher temperatures no optical dichroism could be induced. Table II of Ref. 21, appropriate for randomly oriented centers, will be used for the BT analysis.

B. Features of the polarized resonant Raman spectra

Figure 1 presents the polarized Raman intensities of $F_A(\text{Li}^+)$ under 647.1-, 676.4-, and 752.5-nm exci-

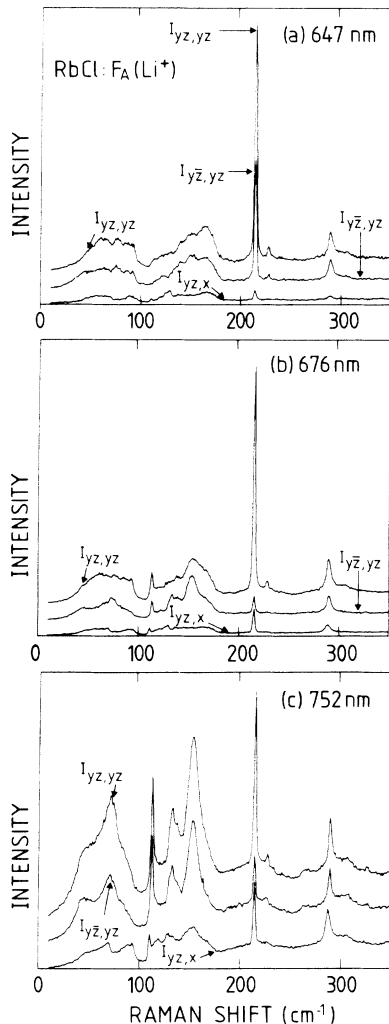


FIG. 1. Frequency dependence of the polarized Raman spectra of $F_A(\text{Li}^+)$ in RbCl at 10 K. The nonzero $I_{yz,x}$ intensity for the high-frequency localized modes is typical for the $F_A(\text{Li}^+)$ off-axis centers. It enhances when the excitation is varied from the F_{A2} to the F_{A1} band [(a)→(c)]. A mode similar to the low-frequency mode at 43 cm^{-1} was also observed for $\text{KCl}:F_A(\text{Li}^+)$. The sharp resonance at 113 cm^{-1} possibly belongs the $F_A(\text{K}^+)$ center.

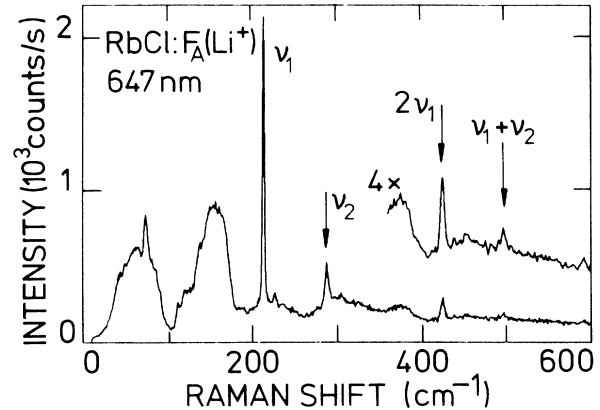


FIG. 2. The overtone and the combination mode of the fundamental modes ν_1 and ν_2 of $F_A(\text{Li}^+)$ in RbCl. The frequency of the overtone $2\nu_1$ is slightly lower than expected in the harmonic approximation.

tation. These wavelengths lie in the F_{A2} band at 636 nm, in between the F_{A1} and F_{A2} band, and in the long-wavelength tail of the F_{A1} band at 721 nm, respectively.^{5,6} After $F \rightarrow F_A(\text{Li}^+)$ conversion, the Raman spectra of $\text{RbCl}:\text{Li}^+$ possess sharp and intense high-frequency modes at 214 and 288 cm^{-1} . Within the F -center-like phonon spectrum²² a narrow resonance at 113 cm^{-1} is observed and a broad one at 43 cm^{-1} with similar properties as the 47-cm^{-1} mode of $F_A(\text{Li}^+)$ in KCl .³ The weak first overtone and the combination mode of the 214- and 288-cm^{-1} modes are also observed (Fig. 2). Except for the 43- and the 113-cm^{-1} modes, the $I_{yz,x}$ and $I_{x,y}$ are nonzero. Figure 3 shows the polarized Raman intensities of the high-frequency mode near 288 cm^{-1} with a resolution of 0.8 cm^{-1} . It illustrates that we deal, in fact, with

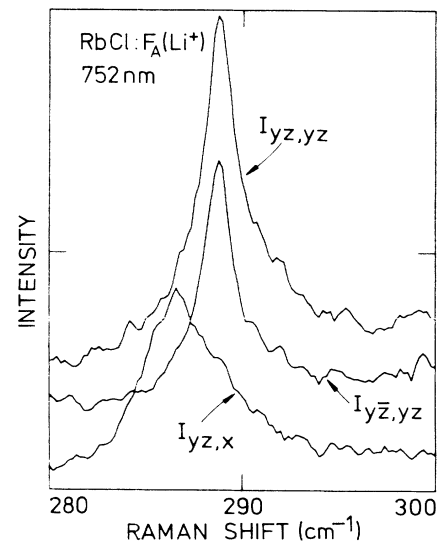


FIG. 3. Polarized Raman spectra of the mode near 288 cm^{-1} of $F_A(\text{Li}^+)$ in RbCl, with a resolution of 0.8 cm^{-1} . We deal, in fact, with two modes possessing different polarization properties.

TABLE I. The ratios of the intensity parameters under 647-, 676-, and 752-nm excitation, which can be retrieved from the polarized Raman intensities of Figs. 1(a), 1(b), and 1(c), respectively.

Mode (cm^{-1})	647 nm		676 nm		752 nm	
	$\frac{s_{21}}{q_2 + s_{11}}$	$\frac{r_1 + s_{12}}{q_2 + s_{11}}$	$\frac{s_{21}}{q_2 + s_{11}}$	$\frac{r_1 + s_{12}}{q_2 + s_{11}}$	$\frac{s_{21}}{q_2 + s_{11}}$	$\frac{r_1 + s_{12}}{q_2 + s_{11}}$
43			≤ 0.15		≤ 0.08	≤ 0.12
113			≤ 0.03	0.25 ± 0.03	≤ 0.05	0.12 ± 0.02
214	0.02 ± 0.01	0.36 ± 0.05	0.09 ± 0.02	0.87 ± 0.04	0.28 ± 0.05	0.63 ± 0.07
288.5	≤ 0.07	0.18 ± 0.04	≤ 0.15	0.26 ± 0.04	≤ 0.35	0.18 ± 0.04

two modes, possessing different polarization properties. Whereas for the mode at 288.5 cm^{-1} $I_{yz,yz}$ and $I_{y\bar{z},yz}$ are dominant, the one at 286.5 cm^{-1} possesses exclusively nonzero $I_{yz,x}$. The intensity parameters (1) of the Raman modes at 47, 113, 214, and 289 cm^{-1} are summarized in Table I for three excitation wavelengths. Due to the overlap with the 286.5-cm^{-1} mode in the $I_{yz,x}$ spectrum, the s_{21} parameter of the 288.5-cm^{-1} mode cannot be obtained accurately. The peak height is given as an upper limit.

For KF the Raman spectra of $F_A(\text{Li}^+)$ are measured for a number of laser lines in the wavelength range from 454.5 to 530.9 nm. This is at resonance with the F_{A1} and F_{A2} absorption bands, which have their maxima at 525 and 429 nm, respectively.^{23,24} The polarized Raman intensities, $I_{x,x}$ and $I_{x,y}$, under 488.0-nm excitation are presented in Fig. 4. The Raman spectra exhibit localized vibrations at 352 and 394 cm^{-1} . A low-frequency mode, such as for $F_A(\text{Li}^+)$ in KBr, KCl, and RbCl, is not observed in the Raman spectrum of $\text{KF}:F_A(\text{Li}^+)$.

The features of the high-frequency modes of $F_A(\text{Li}^+)$ in RbCl and KF are very similar in several ways: (i) The position of the modes near 288 and 394 cm^{-1} is slightly different for perpendicular ($I_{x,y}$ and $I_{yz,x}$) and parallel scattering ($I_{x,x}$ and $I_{yz,yz}$), pointing to two distinct modes; (ii) both high-frequency modes possess nonzero

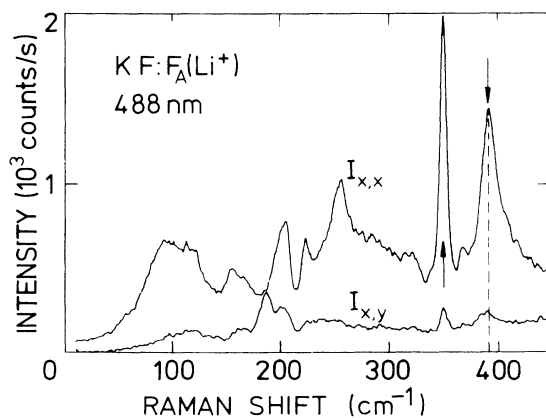


FIG. 4. Polarized Raman spectra of $F_A(\text{Li}^+)$ in KF at 10 K under 488-nm excitation. Apart from the absence of a low-frequency resonance, the Raman spectra of $\text{KF}:F_A(\text{Li}^+)$ are very similar to those of $F_A(\text{Li}^+)$ in KCl and RbCl. The mode at 390 cm^{-1} in the $I_{x,y}$ spectrum nearly coincides with the 394-cm^{-1} mode in the $I_{x,x}$ spectrum.

s IP's; (iii) these s IP's are considerably larger under F_{A1} than under F_{A2} excitation; (iv) the localized modes with the lowest frequency, i.e., the 214- and 352-cm^{-1} modes, are most pronounced under F_{A2} excitation; (v) they are accompanied by a much weaker mode at 226 and 370 cm^{-1} , respectively. Except for (v), the same properties are observed for the high-frequency Li^+ vibrations in the Raman spectra of $F_A(\text{Li}^+)$ in *additively colored* $\text{KCl}:\text{Li}^+$.^{3,22}

The polarized resonant Raman spectra of $F_A(\text{Li}^+)$ in NaCl under 488.0-nm excitation are shown in Fig. 5. They differ from the Raman spectra of the F -center by an intense mode at 264 cm^{-1} in the high-frequency tail of the phonon spectrum. This mode exhibits zero $I_{yz,x}$. The resonant modes of the F center at 160 and 181 cm^{-1} shift to 154 and 183 cm^{-1} for $F_A(\text{Li}^+)$, similar to the case of $F_A(\text{Li}^+)$ in KBr.⁸ For different excitation frequencies at resonance with the unresolved $F_A(\text{Li}^+)$ absorption band at 460 nm, the polarized Raman spectra of $\text{NaCl}:F_A(\text{Li}^+)$ are essentially mutually identical.

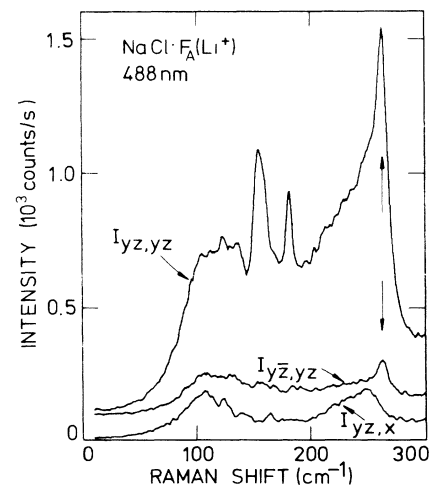


FIG. 5. In contrast to the off-axis $F_A(\text{Li}^+)$ centers, the polarized Raman spectra of $\text{NaCl}:F_A(\text{Li}^+)$ exhibit only one high-frequency mode, which possesses zero $I_{yz,x}$. The resonant modes of the F center in NaCl are shifted to 154 and 183 cm^{-1} for $F_A(\text{Li}^+)$. The polarized Raman spectra remain essentially unchanged when the excitation is tuned through the F_A -absorption spectrum.

C. Identification of the $F_A(\text{Li}^+)$ -induced modes in RbCl

It has been shown that the highly preferential alignment of the $F_A(\text{Li}^+)$ centers diminishes the resonant contribution to the Raman spectrum.³ As such, even small concentrations of other defect centers may have a non-negligible contribution to the Raman spectrum. Since the RbCl:Li⁺ samples contain a certain amount of K⁺, the identification of the $F_A(\text{Li}^+)$ -induced vibrational features needs some comment.

As witnessed by their combination mode, the modes at 214 and 288 cm⁻¹ belong to the same center. The frequency ratio between the 214-cm⁻¹ mode and the weak mode at 226-cm⁻¹ mode is equal to 1.05 and is the same as that observed for the 216-cm⁻¹ mode of $F_A(\text{Li}^+)$ in KCl on ⁷Li⁺ to ⁶Li⁺ substitution. Regardless of the Raman intensity of other modes, the intensity ratio between them is consistently found to be 0.06 ± 0.01 under all excitations, which is very close to the natural abundance ratio of the ⁶Li⁺ and ⁷Li⁺ isotopes. Also, there is a strong correspondence between the 43-, 214-, and 288-cm⁻¹ mode and the $F_A(\text{Li}^+)$ -induced modes in KCl (cf. Sec. IIIA). For these reasons, we associate these three Raman modes with the $F_A(\text{Li}^+)$ center in RbCl. The intensity of the sharp resonance at 113 cm⁻¹, relative to that of the other modes, varies by a factor 2, when other bleaching light is used for $F \rightarrow F_A$ conversion. Therefore, it belongs to another center, possibly $F_A(\text{K}^+)$.

IV. BEHAVIOR-TYPE ANALYSIS AND INTERPRETATION

A. Modes possessing nonzero depolarized scattering

The high-frequency modes of $F_A(\text{Li}^+)$ in RbCl and KF possess nonzero s_i IP's. Since only three independent IP's are left under 676.4-nm excitation, namely $q (= q_i)$, $r + s' (= r_i + s_{i2})$, and $s (= s_{i1} = s_{i3})$, the values in Table I lead to the BT relations:

$$q \neq 0, \quad r + s' = 0.96q, \quad s = 0.1q, \quad (4)$$

$$q \neq 0, \quad 0.25q \leq r + s' \leq 0.31q, \quad 0 \leq s \leq 0.18q, \quad (5)$$

for the 214- and the 288.5-cm⁻¹ mode, respectively. In Table II of Ref. 21 only BT with nonzero q and s have to be considered. BT's 4, 6, and 9 are inconsistent with the observed relations between the IP on the basis of the inequalities for the $r + s'$ parameter. The same conclusion is true for BT's 5 and 6, if we take into account that the polarized Raman data always obey the relation $|s'| \leq s$. Consequently, the IP relations (4) and (5) are consistent with the BT's 1 and 8, which occur for the representative modes

$$\begin{aligned} C_1 : A, \quad C_2[010] : A, \quad C_2[110] : A, \\ D_2[110] : A, \quad C_4[001] : A \end{aligned} \quad (6)$$

This means that the two high-frequency modes point to an off-center position of the Li⁺ ion for $F_A(\text{Li}^+)$ in RbCl.

In this model, they both transform according to the A' representation of the C_{1h} symmetry, belonging to the representative mode $C_2:A$. It is not possible to decide whether the mirror plane is a {110} or a {010} plane. The C_{4v} symmetry group of the on-axis model is not included in (6).

For $F_A(\text{Li}^+)$ in KF only the polarized Raman intensities $I_{x,x}$ and $I_{x,y}$ are measured. From these spectra nonzero q and s IP's are derived for the modes at 352 and 394 cm⁻¹. One can verify that a BT analysis based on of this limited number of IP's is still consistent with the C_{1h} symmetry group of the off-axis model. The irreducible representation of the modes, however, cannot be obtained. Because of the close correspondence between the polarized Raman spectra of $F_A(\text{Li}^+)$ in KF and RbCl (cf. Sec. IIIB), we assume the same interpretation for the 352- and 394-cm⁻¹ modes in KF as for the 214- and 288.5-cm⁻¹ modes in RbCl, respectively.

B. Nature of the Raman modes of an off-axis center

In the preceding section we established the off-axis position of the Li⁺ ion in KF: $F_A(\text{Li}^+)$ and RbCl: $F_A(\text{Li}^+)$, as was already found for $F_A(\text{Li}^+)$ in KCl.³ For RbCl the polarization properties of the Raman modes do not change below 40 K. This demonstrates that $F_A(\text{Li}^+)$ in RbCl is an off-axis center above, as well as below, the temperature where it exhibits the transition from $F_A(\text{I})$ -type to $F_A(\text{II})$ -type center,⁵ and in the temperature range where no electrocaloric effect is observed for the isolated Li⁺ in the same host crystal.^{4,7} This is in agreement with the dielectric measurements under hydrostatic pressure on the isolated Li⁺ center in RbCl⁴ and eliminates the possibility of an on- to off-center transition.

1. The Li⁺ coordinates within the plane of symmetry

We already stressed the correspondence between the properties of the high-frequency modes of $F_A(\text{Li}^+)$ in KCl, RbCl, and KF (cf. Sec. IIIB). The BT analysis also established that the high-frequency modes of RbCl and KF transform according to the same irreducible representation as those observed in KCl.³ In the latter host a normal isotope shift is observed for these modes upon ⁷Li⁺ to ⁶Li⁺ substitution, pointing to Li⁺ vibrations.^{1,12,22} The isotope shift of the 214- and 352-cm⁻¹ modes in RbCl and KF, respectively, was also established, due to the natural abundance of ⁶Li⁺ in the sample. Therefore, we associate the 288.5- and 394-cm⁻¹ mode of $F_A(\text{Li}^+)$ in RbCl and KF with a Li⁺ motion parallel to the defect axis. The modes at 214 and 352 cm⁻¹ represent a Li⁺ vibration perpendicular to the defect axis, but within the symmetry plane of the off-axis model.³

2. The Li⁺ mode perpendicular to the mirror plane

For the KCl:Li⁺ samples a third high-frequency mode is observed at 249 cm⁻¹, possessing a normal shift upon

Li⁺ isotope substitution.²² However, in x-ray irradiated samples this mode is only *marginally* observed under *off-resonance* excitation.³ Hence, it was not certain whether or not it might be attributed to the $F_A(\text{Li}^+)$ center. The difference between the x-ray irradiated and additively colored KCl:Li⁺ crystals can be explained by preferential absorption of the scattered light, which will be discussed in a forthcoming paper. The conclusion is that the measurements on additively colored crystals reveal the actual polarization properties of the $F_A(\text{Li}^+)$ center in KCl. For these measurements the 249-cm⁻¹ mode appears under F_{A1} resonant excitation, as well. The assignment of this mode to the $F_A(\text{Li}^+)$ center is supported by the observation of a similar mode for RbCl: $F_A(\text{Li}^+)$ and KF: $F_A(\text{Li}^+)$.

Since the third Li⁺ mode overlaps the Li⁺ mode parallel to the defect axis, it is difficult to obtain accurate IP's. Nevertheless, the irreducible representation, according to which this mode transforms, can be obtained by elimination. Since the two other Li⁺ modes transform according to $C_{1h}:A'$, the third one necessarily belongs to $C_{1h}:A''$ and describes a Li⁺ motion perpendicular to the mirror plane. The $C_{1h}:A''$ representation stems from the E representation of the higher C_{4v} point group. Within experimental accuracy, the polarization properties of the 249- and 286.5-cm⁻¹ modes in KCl and RbCl, respectively, are indeed consistent with this representation: They both possess zero q and r IP's, and nonzero s . It is interesting to mention that if a nonzero q IP would be observed for the $C_{1h}:A''$ mode, it is possible to eliminate an off-axis displacement of the Li⁺ ion in a {100} plane on the basis of polarized Raman measurements: For the $C_{1h}\{100\}:A''$ representation only off-diagonal Raman-tensor components can be observed, whereas for $C_{1h}\{110\}:A''$ both off- and on-diagonal tensor components can occur.

3. The low-frequency lattice mode

As far as can be verified, the 43-cm⁻¹ mode of $F_A(\text{Li}^+)$ in RbCl possesses $s = 0$ and $r = 0$. The latter is related to the fact that the mode is only observed under F_{A1} excitation. The same properties were observed for the 47-cm⁻¹ mode of $F_A(\text{Li}^+)$ in KCl. It belongs to the $C_{1h}:A'$ representation and is associated to a motion of the ions surrounding the Li⁺ ion, in which the Li⁺ itself does not participate.³

C. Modes possessing zero perpendicular scattering

The following BT relations are established for the 264-cm⁻¹ mode of $F_A(\text{Li}^+)$ in NaCl and the 113-cm⁻¹ mode, observed in the RbCl samples under 676.4-nm excitation, respectively:

$$q \neq 0, \quad r = 0.12q, \quad s = s' = 0, \quad (7)$$

$$q \neq 0, \quad r = 0.77q, \quad s = s' = 0. \quad (8)$$

The zero s/q ratio leads to the same procedure of the BT analysis as that for the $F_A(\text{Li}^+)$ modes in KBr and that

for the 47- and 266-cm⁻¹ mode in KCl: $F_A(\text{Li}^+)$.^{3,8} One concludes that the modes belong to one of the representative symmetries:

$$D_2[100] : A, \quad D_4[001] : A_1. \quad (9)$$

This is consistent with an on-center model, in which the two modes transform according to the $C_{4v}:A_1$ representation.

D. Nature of the Raman modes of an on-axis center

The BT analysis established the on-axis behavior of $F_A(\text{Li}^+)$ in NaCl. It is in agreement with the absence of paraelectric behavior⁷ and the calculations of Sangster²⁵ and of Catlow *et al.*²⁶ for the isolated Li⁺ center in NaCl. The high frequency of the 264-cm⁻¹ mode, which lies very close to the Li⁺ vibrations at 266 and 288.5 cm⁻¹ in KCl and RbCl, respectively, suggests it to be a Li⁺ motion. The $C_{4v}:A_1$ representation, to which it belongs, points to a Li⁺ motion parallel to the defect axis. This was also the only Li⁺ coordinate observed for the on-axis $F_A(\text{Li}^+)$ in KBr.⁸

It was shown in Sec. III C that the 113-cm⁻¹ mode, observed in the RbCl samples, does not belong to the $F_A(\text{Li}^+)$ center. We will tentatively associate it with the $F_A(\text{K}^+)$ center. The C_{4v} symmetry established from the polarized Raman intensities of the 113-cm⁻¹ mode agrees with this assumption. If a K⁺ motion is involved in the 113-cm⁻¹ mode it occurs along the $F_A(\text{K}^+)$ defect axis.

V. DISCUSSION

A. Off-center behavior and F_A type

In Table II the on- or off-axis behavior of $F_A(\text{Li}^+)$ in the investigated host crystals is compared to its $F_A(\text{I})$ or $F_A(\text{II})$ type and with the on- or off-center behavior of the isolated Li⁺ impurity in the corresponding host crystals. Obviously, the on- or off-axis behavior of the isolated impurity is systematically preserved on perturbing it with a nearest-neighbor (NN) F center. Also, the correlation between off-axis behavior and F_A type is confirmed.⁵ The transition from an $F_A(\text{II})$ - to an $F_A(\text{I})$ -type center for $F_A(\text{Li}^+)$ in RbCl with decreasing temperature, which was observed by optical reorientation and luminescence measurements,⁵ is not reflected in the polarized Raman spectra. The transition was attributed to the freezing in of the Li⁺ ion in one of the potential minima. This illustrates that the detection of off-center behavior by means of polarized Raman spectra is independent of the reorientational motion of the Li⁺ dipoles (cf. also Refs. 18 and 19).

B. Vibrational modes versus off-center behavior

The interpretation of the $F_A(\text{Li}^+)$ -induced vibrational modes is summarized in Table III. The available data for the isolated impurity center are also included. Three

TABLE II. Comparison of the on- or off-axis behavior of $F_A(\text{Li}^+)$, as established by our analysis, with its F_A type and with the on- or off-center behavior of the isolated Li^+ impurity in the corresponding host crystals. The same information is given for $\text{RbCl}:\text{K}^+$. The 113-cm^{-1} mode is only tentatively associated with the $F_A(\text{K}^+)$ in RbCl .

	Isolated impurity	F_A center	
	On/off center	On/off axis	F_A type
$\text{NaCl}:\text{Li}^+$	on ^a	on	
$\text{KBr}:\text{Li}^+$	on ^b	on	I ^g
$\text{RbCl}:\text{K}^+$	on ^c	on	I ^g
$\text{KF}:\text{Li}^+$	off ^d	off	II ^h
$\text{KCl}:\text{Li}^+$	off ^e	off	II ^g
$\text{RbCl}:\text{Li}^+$	off ^f	off	I ($T < 15\text{ K}$) ⁱ II ($T > 15\text{ K}$)

^aReferences 7 and 26.

^bReferences 7 and 9.

^cReference 37.

^dReference 26.

^eReferences 26 and 38.

^fReferences 4 and 26.

^gReference 6.

^hReference 23.

ⁱReference 5.

properties of this table need attention: (i) *Low-frequency* Li^+ modes are observed for the isolated Li^+ on centers, whereas the $F_A(\text{Li}^+)$ centers with on-axis behavior possess *high-frequency* modes; (ii) high-frequency Li^+ modes are calculated for the off-center Li^+ in KCl , as well as for the off-axis $F_A(\text{Li}^+)$ centers; (iii) for the $F_A(\text{Li}^+)$ center Li^+ modes perpendicular to the defect axis are only observed if the center exhibits off-axis behavior. The latter feature was explained in Ref. 3 in terms of selective resonant enhancement of the Raman tensor components. As a result, the $C_{4v}:E$ modes of an on-center system are not expected to be resonantly enhanced under excitation of the F_{A1} and F_{A2} absorption bands of $F_A(\text{Li}^+)$.

The calculations of Quigley and Das⁹ predict that at room temperature the isolated Li^+ in KBr is an off-center system like Li^+ in KCl . The observed relations between the vibrational features of $F_A(\text{Li}^+)$ and the Li^+ equilibrium position would be nicely confirmed, if additional high-frequency modes appeared in the Raman spectrum of $F_A(\text{Li}^+)$ in KBr at higher temperatures and if no low-frequency Li^+ vibration would be observed for the isolated Li^+ in KBr . Recently, a similar study of the vibrational features of the Ag^+ impurity in KI has been performed. For this center the on- and off-center position of the impurity ion are observed to occur together in the temperature range between 1.2 and 20 K.^{27,28}

The modes in the first column of Table III are associated to a motion of the ions surrounding the impurity, in which the Li^+ ion hardly participates. It is most extensively investigated for the Li^+ and the $F_A(\text{Li}^+)$ in KCl .^{3,11-14} The occurrence of this mode is not related to on- or off-center behavior. Neither is there a clear correspondence on this point between the isolated Li^+ and the $F_A(\text{Li}^+)$ center. A model calculation showed that the small anomalous isotope shift of the low-frequency mode of the Li^+ and the $F_A(\text{Li}^+)$ in KCl possibly results from weak coupling to the tunneling motion of the impurity ion.²⁹ Consistent with this explanation, the 28-

cm^{-1} mode of the $F_A(\text{Li}^+)$ on-center in KBr possesses no isotope shift.¹² It is indicated to check the shift of the 43-cm^{-1} mode of $\text{RbCl}:F_A(\text{Li}^+)$ upon isotope substitution: Although the Li^+ equilibrium position is off axis in this case, the impurity ion is not expected to exhibit quantum-mechanical tunneling.^{4,5}

C. Einstein-oscillator frequencies of the Li^+ modes

The frequency ratio $\nu(^6\text{Li}^+)/\nu(^7\text{Li}^+)\approx 1.08$ of the $F_A(\text{Li}^+)$ modes in KCl and KBr parallel to the defect axis,^{1,12} suggests regarding the modes as Li^+ vibrations in a rigid lattice. The Einstein-oscillator frequencies

$$\omega = \left(\frac{k}{m}\right)^{1/2}, \quad \omega = \left(\frac{2k}{m}\right)^{1/2} \quad (10)$$

for $F_A(^7\text{Li}^+)$ and the isolated $^7\text{Li}^+$ center, respectively, are presented for different host crystals in Table IV, together with the experimental frequencies of the $^7\text{Li}^+$ modes. For the $F_A(\text{Li}^+)$ mode parallel to the defect axis, the force constant is taken equal to zero at the side of the anion vacancy. For the Li^+ -halogen-ion interaction in a certain host the effective force constant k of the corresponding lithium halide crystal is used. As such, it is implicitly assumed that the Li^+ -NN distance is equal to the lattice parameter of the lithium halide.

For all cases the Einstein oscillator model works reasonably well, except for the isolated Li^+ impurity with on-center behavior. Note also the correspondence for the 113-cm^{-1} mode, tentatively attributed to the $F_A(\text{K}^+)$ center in RbCl . For the $F_A(\text{Li}^+)$ center the model agrees with (i) an increased frequency with decreasing halogen size, which is only slightly dependent on the alkali ion and the lattice parameter of the host lattice (cf. the lithium chlorides); and (ii) with the observation of a *high-frequency* Li^+ mode along the defect axis for both on- and off-axis systems.

TABLE III. Classification of the vibrational modes induced by the isolated Li^+ and the $F_A(\text{Li}^+)$ center in alkali halides according to their frequency and the vibrational coordinate. For the off-axis $F_A(\text{Li}^+)$ centers the Li^+ motion is classified according to its direction with respect to the defect axis, as well as with respect to the off-axis displacement. The 113-cm^{-1} mode is tentatively associated with the $F_A(\text{K}^+)$ center in RbCl .

Defect system	On/off center	Low frequency (cm^{-1})		High-frequency impurity mode (cm^{-1})		
		lattice mode	impurity mode	\parallel off-center displacement	\perp off-center displacement	\parallel defect axis
$\text{KCl}:\text{Li}^+$	off	42, ^a 44 ^b		280 ^f		380 ^f
$\text{NaCl}:\text{Li}^+$	on	140 ^c	43.7 ^a			
$\text{KBr}:\text{Li}^+$	on		16.3 ^a			
	On/off axis	lattice mode		\perp defect axis	\perp defect axis	\parallel defect axis
$\text{KF}:F_A(\text{Li}^+)$	off			352	390	394
$\text{RbCl}:F_A(\text{Li}^+)$	off	43		214	286.5	288.5
$\text{KCl}:F_A(\text{Li}^+)$	off	47 ^d		216 ^d	249 ^d	266 ^d
$\text{NaCl}:F_A(\text{Li}^+)$	on					264
$\text{KBr}:F_A(\text{Li}^+)$	on	28 ^e				227 ^e
$\text{RbCl}:F_A(\text{K}^+)$	on					113

^aReference 11.

^bReferences 12 and 14.

^cReference 39.

^dReferences 1, 3, and 22.

^eReferences 8 and 12.

^fTheoretically calculated (Ref. 13.)

D. High-frequency Li^+ modes and lattice relaxation

The small Li^+ size results in a tendency of the Li^+ impurity to relax towards its NN. If this tendency is not too strong, the isolated Li^+ impurity remains on center. The Li^+ —NN distance is equal to the host-lattice parameter and thus considerably larger than was assumed in the Einstein-oscillator model. In these cases the ac-

tual force constant determining the Li^+ vibration is very much smaller than the force constant of lithium halide.³⁰ As a result, the Li^+ modes of an isolated Li^+ on center are expected to possess a much lower frequency than the estimated one in Table IV. Off-center displacement of the Li^+ impurity is accompanied by a relaxation of the NN halogen ions.^{25,13} This effectively decreases the Li^+ —NN distance, resulting in the estimated high-frequency Li^+ vibrations.

In this picture, the high frequency of the Li^+ mode parallel to the $F_A(\text{Li}^+)$ defect axis for on-axis as well as for off-axis systems can be understood, if a relaxation of the Li^+ equilibrium position is assumed. The distance between the Li^+ position and the NN halogen site, opposite to the adjacent F center, should equal the lattice parameter of lithium halide (cf. Fig. 6). ENDOR measurements on $F_A(\text{Li}^+)$ in KCl (Ref. 31) confirm this Li^+ relaxation parallel to the defect axis, which is allowed by the small Li^+ size and its asymmetric surrounding in $F_A(\text{Li}^+)$. For $F_A(\text{Li}^+)$ in KCl , RbCl , and KF an additional displacement of the Li^+ ion occurs perpendicular to the defect axis. The relaxation of the impurity in the F_A center is opposite to that established for the $\text{Tl}^0(1)$ center.^{32,33} The Tl^+ ion, however, is as big as K^+ . For an F_A -like center the Tl^+ ion in KCl would stay on the substitutional site. However, the trapped electron is not localized in the anion vacancy, but on the Tl^+ ion. The ground electronic p state points along the defect axis, thus pushing the impurity towards the vacancy. In the first excited electronic p state, which is directed perpendicular to the defect axis, the Tl atom occupies the sub-

TABLE IV. Einstein-oscillator frequencies (ω_E) for the Li^+ modes of $F_A(\text{Li}^+)$ and the isolated Li^+ center compared with the experimentally observed or the theoretically calculated ones. The force constants of the Li^+ modes are taken equal to that of the corresponding lithium halide. The 113-cm^{-1} mode is tentatively associated with $\text{RbCl}:F_A(\text{K}^+)$.

Defect system	On/off center	Li^+ mode (cm^{-1})	ω_E (cm^{-1})
$\text{KF}:F_A(\text{Li}^+)$	off	394	400
$\text{RbCl}:F_A(\text{Li}^+)$	off	288.5	285
$\text{KCl}:F_A(\text{Li}^+)$	off	266 ^a	285
$\text{NaCl}:F_A(\text{Li}^+)$	on	264	285
$\text{KBr}:F_A(\text{Li}^+)$	on	227 ^b	266
$\text{RbCl}:F_A(\text{K}^+)$	on	113	108
$\text{KCl}:\text{Li}^+$	off	380 ^c	403
$\text{NaCl}:\text{Li}^+$	on	43.7 ^d	403
$\text{KBr}:\text{Li}^+$	on	16.3 ^d	376

^aReferences 1, 3, and 12.

^bReferences 8 and 12.

^cReference 13.

^dReference 11.

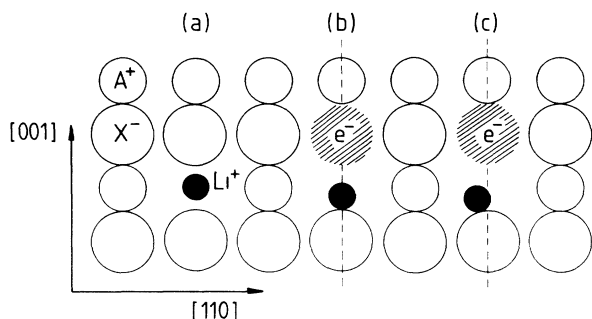


FIG. 6. (a) Schematic picture in a {110} crystal plane of the isolated Li^+ impurity with on-center behavior. (b) For the $F_A(\text{Li}^+)$ center, the Li^+ equilibrium position relaxes parallel to the defect axis and away from the adjacent F center. (c) For an off-axis center also an additional relaxation perpendicular to the defect axis occurs. The ionic radii are representative for $\text{RbCl}:\text{Li}^+$.

stitutional site. A similar situation takes place for the F center: The larger radial extension of the relaxed excited state results in an outward relaxation of the NN cations.³⁴ This is also accompanied by a higher frequency of the NN-cation breathing mode.³⁵

In fact, the localized modes of the isolated Li^+ should not be compared with the $F_A(\text{Li}^+)$ modes parallel to the defect axis, but to the modes perpendicular to it. For $F_A(\text{Li}^+)$ centers with off-axis behavior the latter modes are representative for the predicted high-frequency modes of the isolated Li^+ in KCl .¹³ For both $F_A(\text{Li}^+)$ and the isolated Li^+ the vibration of the impurity ion parallel to the off-center displacement exhibits the lowest frequency. The smaller frequency of these modes for $F_A(\text{Li}^+)$ could be related to a smaller off-center displacement and/or a smaller relaxation of the NN ions than for the isolated impurity center.

E. Anharmonicity of the Li^+ potential

Sangster and Stoneham pointed out that their calculations are performed in the harmonic approximation and that the effective local-mode frequencies could well be altered for a light impurity in a highly anharmonic potential well.¹³ The anharmonicity of the Li^+ potential of the isolated Li^+ on center in KBr was already discussed in Refs. 8, 11, and 36. The occurrence of higher-order Raman scattering for $F_A(\text{Li}^+)$ in RbCl enables one to study the anharmonicity of the Li^+ modes for off-center systems too. The isotope shift of the Li^+ mode at $213.5 \pm 0.4 \text{ cm}^{-1}$, parallel to the off-axis displacement, is smaller than that for an Einstein oscillator. This is in contrast to the case of a harmonic oscillator with incipient Gaussian barrier, such as in $\text{KBr}:\text{Li}^+$.³⁶ The first overtone of this mode, at $425.3 \pm 0.4 \text{ cm}^{-1}$, is slightly less than expected in the harmonic approximation. Therefore, fourth-order static anharmonicity would soften the Li^+ potential at large vibrational amplitudes. The strong enhancement of the repulsive forces at shorter distances

would rather result in a hardening. Third-order anharmonicity, treated to second-order perturbation, also leads to a frequency decrease of the overtone frequencies. This reflects again the symmetry lowering due to the off-axis displacement. Nevertheless, the frequency of the lowest vibrational levels is only slightly influenced by the anharmonicity of the Li^+ potential.

VI. CONCLUSIONS

As was already established for KCl and KBr , the $F_A(\text{Li}^+)$ center in RbCl , NaCl , and KF possesses the same on- or off-center behavior as the isolated Li^+ impurity in the corresponding host crystals. In particular, the off-axis behavior of $F_A(\text{Li}^+)$ in RbCl is demonstrated, whereas no changes in the polarized Raman spectra are observed at higher temperatures, where the Li^+ ion has been suggested to be mobile between the equivalent off-axis equilibrium positions at low temperatures. For both on- and off-axis systems, high-frequency vibrations are observed above the phonon cutoff frequency. They can be attributed to the Li^+ coordinate parallel to the $F_A(\text{Li}^+)$ defect axis and the two Li^+ coordinates perpendicular to it. Whereas the former is observed in all cases, the latter occur only for the off-axis centers. In the latter case a Li^+ mode within the mirror plane of the off-axis model and a Li^+ mode perpendicular to it can be distinguished. In some of the hosts the $F_A(\text{Li}^+)$ center also possesses a low-frequency mode, similar to that of the isolated Li^+ center in KCl . It is associated to a motion of the ions surrounding the impurity. The occurrence of this mode is not correlated to on- or off-axis behavior.

The most striking difference between the vibrational features of the isolated Li^+ center and those of $F_A(\text{Li}^+)$ is that they possess *low-* and *high-frequency* Li^+ modes, respectively. A simple Einstein-oscillator model suggests that the occurrence of high-frequency Li^+ vibrations is related to ionic relaxation of the Li^+ itself and/or its environment. This agrees with the theoretically predicted high-frequency modes for the off-center Li^+ in KCl . The Li^+ vibrations perpendicular to the defect axis of the off-axis $F_A(\text{Li}^+)$ centers are representative for the calculated modes. Higher-order scattering from the off-axis $F_A(\text{Li}^+)$ center in RbCl reveals that in this case the frequency of the Li^+ vibrations is barely affected by anharmonicity. The high frequency of the $F_A(\text{Li}^+)$ modes parallel to the defect axis arises from a relaxation of the Li^+ equilibrium position parallel to the defect axis, away from the adjacent F center.

ACKNOWLEDGMENTS

The authors wish to thank G. Baldacchini for supplying the $\text{RbCl}:\text{Li}^+$ samples and A. Bouwen for expert experimental assistance. Financial support from the NFWO (National Fund for Scientific Research, Belgium) for M.L. is gratefully acknowledged. This work was supported by NFWO and IIKW (Interuniversitair Instituut voor Kernwetenschappen, Belgium).

- *Present address: F.O.M. Instituut voor Atoom- en Molecuulfysica, Kruislaan 407, 1098 SJ Amsterdam, The Netherlands.
- ¹B. Fritz, in *Localized Excitations in Solids*, edited by F. Wallis (Plenum, New York, 1968), p. 496.
 - ²F. Rosenberger and F. Lüty, *Solid State Commun.* **7**, 983 (1969).
 - ³M. Leblans, W. Joosen, E. Goovaerts, and D. Schoemaker, *Phys. Rev. B* **35**, 2405 (1987).
 - ⁴K. Thörmer and F. Lüty, *Phys. Status Solidi B* **90**, 277 (1978).
 - ⁵G. Baldacchini, E. Giovenale, F. De Matteis, A. Scacco, F. Somma, M. Casalboni, and U. M. Grassano, *Europhys. Lett.* **7**, 647 (1988).
 - ⁶F. Lüty, in *Physics of Color Centers*, edited by W. B. Fowler (Academic, New York, 1968), p. 181.
 - ⁷S. Kapphan, Ph. D. thesis, University of Utah (1970).
 - ⁸M. Leblans, W. Joosen, D. Schoemaker, A. Mabud, and F. Lüty, *Phys. Rev. B* **39**, 8657 (1989).
 - ⁹R. J. Quigley and T. P. Das, *Phys. Rev.* **177**, 1340 (1969).
 - ¹⁰B. P. Clayman, I. G. Nolt, and A. J. Sievers, *Phys. Rev. Lett.* **19**, 111 (1967).
 - ¹¹A. S. Barker Jr. and A. J. Sievers, *Rev. Mod. Phys.*, Suppl. **2** **47**, 106 (1975).
 - ¹²A. Mabud and F. Lüty, *Abstract Book of the International Conference on Defects in Insulating Crystals, Salt Lake City, 1984* (unpublished), pp. 299 and 301.
 - ¹³M. J. L. Sangster and A. M. Stoneham, *Phys. Rev. B* **26**, 1028 (1982).
 - ¹⁴W. Joosen, E. Goovaerts, and D. Schoemaker, *Phys. Rev. B* **34**, 1273 (1986).
 - ¹⁵J. F. Zhou, E. Goovaerts, and D. Schoemaker, *Phys. Rev. B* **29**, 5509 (1984).
 - ¹⁶E. Goovaerts, J. F. Zhou, W. Joosen, and D. Schoemaker, *Cryst. Lattice Defects Amorph. Mater.* **12**, 317 (1985).
 - ¹⁷W. Joosen and D. Schoemaker, *J. Phys. Chem. Solids* (to be published).
 - ¹⁸H. Fleurent, W. Joosen, and D. Schoemaker, *Phys. Rev. B* **38**, 6257 (1988).
 - ¹⁹H. Fleurent, W. Joosen, and D. Schoemaker, *Phys. Rev. B* **39**, 10 409 (1989).
 - ²⁰M. Leblans, Licentiate thesis, University of Antwerp (1985), and Ph.D. thesis, University of Antwerp (1990).
 - ²¹W. Joosen, E. Goovaerts, and D. Schoemaker, *Phys. Rev. B* **35**, 8215 (1987).
 - ²²D. S. Pan and F. Lüty, in *Proceedings of the Third International Conference on Light Scattering in Solids, Campinas, Brazil, 1975*, edited by M. Balkanski, R. C. C. Leito, and S. P. S. Porto (Flammarion, Paris, 1975), p. 539.
 - ²³L. F. Mollenauer, B. A. Hatch, D. H. Olson, and H. J. Guggenheim, *Phys. Rev. B* **12**, 731 (1975).
 - ²⁴W. C. Collins and I. Schneider, *J. Phys. Chem. Solids* **37**, 917 (1976).
 - ²⁵M. J. L. Sangster, *J. Phys. C* **13**, 5279 (1980).
 - ²⁶C. R. A. Catlow, K. M. Diller, M. J. Norgett, J. Corish, B. M. Parker, and P. W. M. Jacobs, *Phys. Rev. B* **18**, 2739 (1978).
 - ²⁷A. J. Sievers and L. H. Greene, *Phys. Rev. Lett.* **52**, 1234 (1984).
 - ²⁸J. B. Page, J. T. McWhirter, A. J. Sievers, H. Fleurent, A. Bouwen, and D. Schoemaker, *Phys. Rev. Lett.* **63**, 1837 (1989).
 - ²⁹M. Van Himbeek, H. De Raedt, W. Joosen, and D. Schoemaker, *Europhys. Lett.* **4**, 141 (1987).
 - ³⁰G. Benedek and G. F. Nardelli, *J. Chem. Phys.* **48**, 5242 (1968).
 - ³¹R. L. Mieher, *Phys. Rev. Lett.* **8**, 362 (1962).
 - ³²F. J. Ahlers and J.-M. Spaeth, *J. Phys. C* **19**, 4693 (1986).
 - ³³M. Fockele, F. J. Ahlers, F. Lohse, J.-M. Spaeth, and R. H. Bartram, *J. Phys. C* **18**, 1963 (1985).
 - ³⁴R. F. Wood and H. W. Joy, *Phys. Rev.* **136**, A451 (1964).
 - ³⁵B. Fowler, in *Physics of Color Centers*, edited by W. B. Fowler (Academic, New York, 1968), p. 53.
 - ³⁶B. P. Clayman, R. D. Kirby, and A. J. Sievers, *Phys. Rev. B* **3**, 1351 (1971).
 - ³⁷R. J. Rollefson, *Phys. Rev. B* **5**, 3235 (1972).
 - ³⁸O. Pohl and G. Lombardo, *Phys. Rev. Lett.* **15**, 291 (1965).
 - ³⁹M. Möller and R. Kaizer, *Phys. Status Solidi B* **50**, 155 (1972).